Bulletin of the Seismological Society of America, Vol. 106, No. 1, pp. 1–12, February 2016, doi: 10.1785/0120150192

Development of an Earthquake Early Warning System Based on Earthworm: Application to Southwest Iberia

by Núria Romeu Petit, Yolanda Colom Puyané, José Antonio Jara Salvador, Xavier Goula Suriñach, and Teresa Susagna Vidal

Abstract The main aim of this study is to demonstrate the feasibility of an earthquake early warning system (EEWS) to warn of potentially destructive earthquakes in the Cape San Vicente (SV) and Gulf of Cádiz (GC) areas in the southwest Iberian Peninsula, based on real-time broadband stations existing in the region. Historic earthquakes in this region include the 1755 Lisbon (M_w 8.5) and 1969 SV (M_w 7.8) events. This study illustrates the design, configuration, and first results of an EEWS prototype based on the U.S. Geological Survey Earthworm tools and developed at the Institut Cartogràfic i Geològic de Catalunya (ICGC). System main functionalities are real-time data acquisition, processing (*P*-wave picking, event detection, earthquake hypocentral location, and magnitude estimation from previously calculated peak displacement [P_d] and predominant period τ_c of the *P*-wave signal), data archiving, and earthquake early warning dissemination. The prototype was put into operation after a setup period, during which several simulations were carried out to establish the optimal settings. After the first year of operation, one felt earthquake occurred in the area of study. Location and magnitude results are fairly good, compared with the Instituto Geográfico Nacional (IGN) catalog. Lead times obtained are on the order of tens of seconds for the majority of targets, which are long enough to mitigate damage for a large area of the southern coasts of Portugal and Spain due to the GC and SV earthquakes. Preliminary results for this prototype demonstrate the possibility of a regional, reliable, and effective EEWS in southwest Iberia.

Introduction

Despite the global effort into investigating the nucleation processes of earthquakes, these events still appear to strike suddenly and without obvious warning. However, earthquake early warning systems (EEWSs) can help to reduce losses caused by destructive earthquakes (Allen and Kanamori, 2003). The last two decades have seen acceleration in the development and implementation of such systems. EEWSs are operational in several seismically active regions around the world, such as Taiwan (Wu and Teng, 2002; Wu and Zhao, 2006; Hsiao *et al.*, 2009; Chen *et al.*, 2015), Japan (Nakamura, 1984, 1988; Odaka *et al.*, 2003; Horiuchi *et al.*, 2005; Nakamura and Saita, 2007; Hoshiba *et al.*, 2008; Brown *et al.*, 2009; Kamigaichi *et al.*, 2009), and Mexico (Espinosa-Aranda *et al.*, 2009), and they are under development in California (Allen and Kanamori, 2003; Allen *et al.*, 2009; Böse *et al.*, 2009), southern Italy (Zollo *et al.*, 2006; Zollo, Iannaccone, Convertito, *et al.*, 2009; Zollo, Iannaccone, Lancieri, *et al.*, 2009), Turkey (Erdik *et al.*, 2003; Alcik *et al.*, 2009), China (Peng *et al.*, 2011), Romania (Wenzel *et al.*, 1999; Böse *et al.*, 2007; Ionescu *et al.*, 2007), and Switzerland (Cua and Heaton, 2007).

Most EEWSs are conceived as either regional (network-based) or on-site (stand-alone) systems (Kanamori, 2005). In this study, we focus on regional EEWSs, which are based on a seismic network that covers a portion of an area that is exposed to major earthquakes. An event location is computed, and its magnitude is estimated from the early portion of the *P* waves based on previous studies of the properties of seismic waves (Nakamura, 1988; Espinosa-Aranda *et al.*, 1995; Allen and Kanamori, 2003; Kanamori, 2005; Wu and Kanamori, 2005a,b, 2008a,b; Wu *et al.*, 2006, 2007; Zollo *et al.*, 2006; Böse *et al.*, 2007, 2008; Cua and Heaton, 2007; Shieh *et al.*, 2008; Yamada and Heaton, 2008; Köhler *et al.*, 2009; Satriano *et al.*, 2011; Carranza *et al.*, 2013).

An optimally performing EEWS can be defined as a system that provides the largest lead time (i.e., the time interval between the notification of the event and the arrival of the damaging waves at a location) and the minimum errors of the hypocenter location and magnitude estimation. The "blind zone" is the region where the lead time is less than or equal to zero. This study describes the development using Earthworm tools from the U.S. Geological Survey (USGS) of a prototype of a regional EEWS producing a location scenario as a plot of the blind zone and the lead times to specific targets, as a preliminary step to produce a complete scenario with potential damages. As a basis for this development,

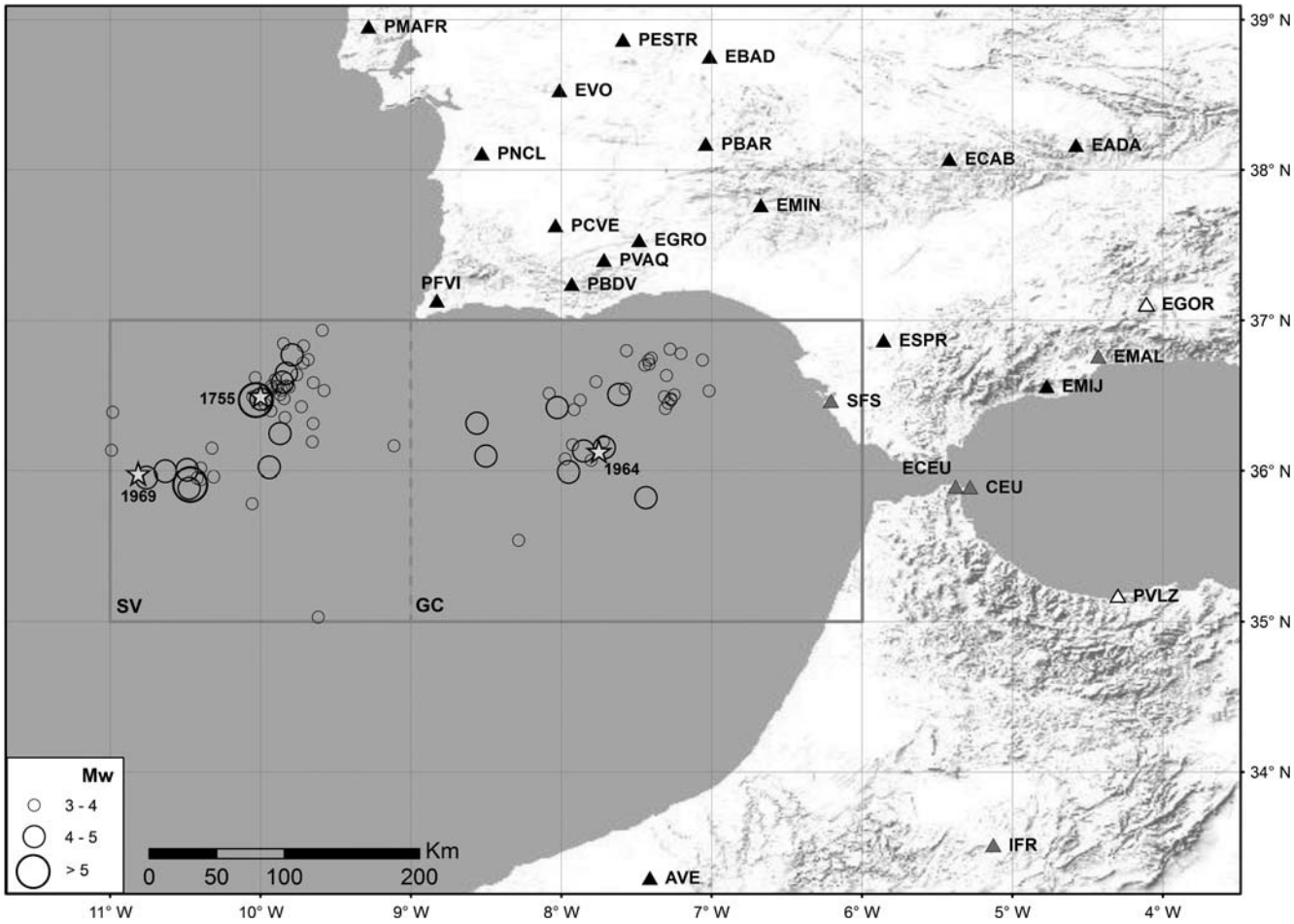

Figure 1. Historical and recent seismicity of the southwest Iberian Peninsula as illustrated by 3 historical earthquakes (1755, 1969, and 1964, represented by stars) and 84 representative earthquakes that occurred between 2006 and 2011 with moment magnitudes from 3.1 to 6.1 from the Instituto Geográfico Nacional (IGN) catalog (represented by circles with areas proportional to M_w) used to configure the prototype earthquake early warning systems (EEWS). Triangles represent the 24 available real-time broadband stations around the study area, which belong to three institutions: Instituto Português do Mar e da Atmosfera (IMPA), IGN, and Real Observatorio de la Armada/Universidad Complutense de Madrid (ROA/UCM). Stations with a final picking configuration are depicted in black, stations with a tentative picking configuration are depicted in gray, and rejected stations are shown as white triangles. The gray square surrounds the study area, which includes the Cape San Vicente (SV) and Gulf of Cádiz (GC) seismogenic zones, separated by a vertical dashed line (9° W).

we use the Earthworm-based automatic seismic detection system, which has been operational at the regional seismic network of Catalonia since 2005 (Goula *et al.*, 2001; Romeu *et al.*, 2006). Finally, this EEWS has been installed as part of a test within the southwest Iberian Peninsula area using the currently available real-time seismic stations in the region. Although currently the system is still undergoing testing, after one year of operation results are promising.

The south Iberian Peninsula is located near a complex plate boundary between Eurasia and Africa. This boundary is commonly divided into three sections (Buforn *et al.*, 1988). In the central section, which is east of 16° W, deformation is distributed over a large area that extends 300 km from north to south near the continental margin of the Iberian Peninsula (Chen and Grimison, 1989). Seismicity is scattered in this central section, and most events are concentrated along a 100-km-wide band that trends east-southeast–west-northwest from 16° W to 9° W. Seismicity in the Gulf of Cádiz (GC) is more dense to the north around Guadalquivir bank. The seismicity is characterized by moderate earthquakes at shallow depths ($h < 40$ km), as well as intermediate depth (40–150 km) and some very deep events (650 km) (Buforn *et al.*, 1988, 2004). Several very large earthquakes have also occurred, especially offshore Cape San Vicente (SV) and in the GC (Fig. 1). The largest one, the 1755 M_w 8.5 Lisbon earthquake, was associated with a large tsunami and caused more than 60,000 casualties and significant damage in the southwest Iberian Peninsula and northwest Morocco (Buforn *et al.*, 1988; Baptista *et al.*, 2003; Gutscher *et al.*, 2006; Grandin *et al.*, 2007). This was not an isolated event; there are references to other large earthquakes since the Roman age. The largest instrumental earthquake in recent times (M_w 7.8) occurred on 28 February 1969 in the eastern Horseshoe abyssal plain (Grimison and Chen, 1986). In the GC, seismicity is concentrated around Guadalquivir bank; the occurrence of an M_w 6.2 earthquake in 1964 (Udias and López-Arroyo, 1970;

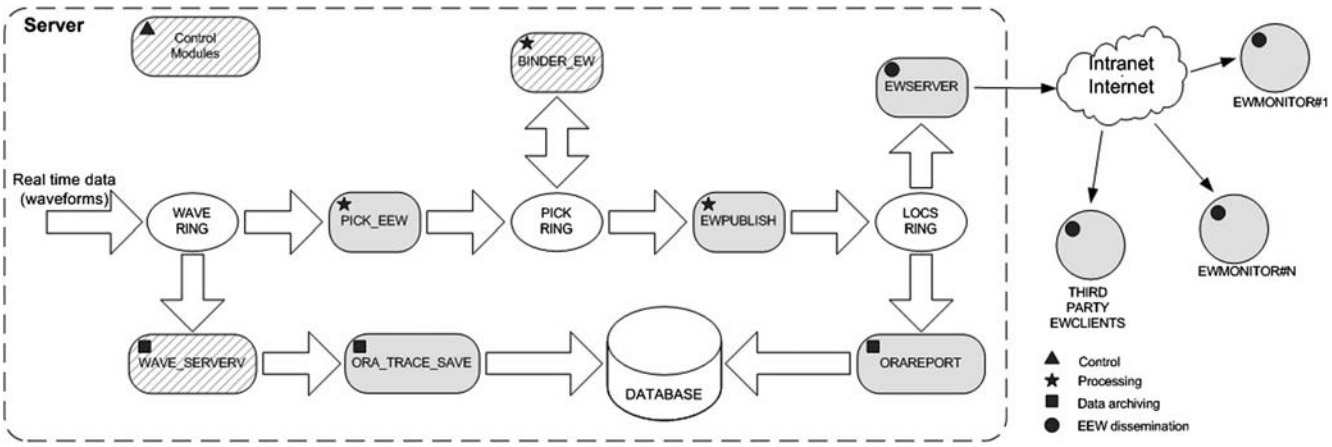

Figure 2. The EEWS prototype based on Earthworm (Johnson *et al.*, 1995). The symbols in the modules indicate their functionalities: triangle, control; star, processing; square, data archiving; and circle, EEW dissemination modules. Striped backgrounds are the original form of Earthworm, and shaded modules are those specially created or modified from Earthworm for the prototype.

Buforn *et al.*, 1988) suggests that this structure, which is clearly identified on seismic profiles and free-air gravity anomaly maps (Gràcia *et al.*, 2003), is active. The past and recent seismicity in this central section of the plate boundary and the existence of areas of potential damage make this region suitable for the implementation of an EEWS.

System Architecture

The proposed EEWS prototype was based on Earthworm for three main reasons. First, it is an adaptable open source. Second, its reliability has been demonstrated by the Automatic Determination System at Institut Cartogràfic i Geològic de Catalunya (ICGC) (Goula *et al.*, 2001; Romeu *et al.*, 2006), which is based on the Earthworm code (Johnson *et al.*, 1995); it has been operating and evolving since 2005 and serves as a rapid alert system in Catalonia, northeast Spain, and southern France (Goula *et al.*, 2008). Third, the USGS developed Earthworm as a modular system; this means that each function of the system is performed by a program that can work independently of the other modules. Each module communicates with the others using shared memory regions, called transport rings, by messages that can contain information about waveforms, picks, events, magnitudes, and so on. Thus, the schema of the system can be easily customized using a proper subset of modules (Olivieri and Clinton, 2012).

An EEWS will likely have the following functionalities: data acquisition, processing, data archiving, EEW dissemination, and state-of-health control. The main modules in our prototype are shown in Figure 2; some of them are originally from Earthworm, whereas others have been slightly modified, adapted, or created (Table 1). The criteria used to choose, modify, or create modules and their configurations are the optimization of the time required to obtain a first location and estimated magnitude of an acceptable quality and the requirement to update the location and estimated magnitude whenever a new arrival time is detected and associated with the event. More precisely, the hypocenter and origin time obtained will be acceptable if their errors have a low impact (i.e., less than 10%) on the warning time. About the estimated magnitude, a tolerable error would have to be less than ± 0.5. For this reason, the design of the prototype is focused on the processing modules (i.e., PICK_EEW, BINDER_EW, and EWPUBLISH).

Offline Data Set and Seismic Network

Offline data were compiled to configure the system (basically PICK_EEW and BINDER_EW modules) and optimize its functionality (Pazos *et al.*, 2015). We considered the seismic zone delimitated by the grid (35°–37° N, 11°–6° W) and took into account the existing and available 24 real-time seismic stations in the southwest of the Iberian Peninsula and Morocco (Fig. 1), which belong to the three institutions involved in the ALERT-ES project: Instituto Português do Mar e da Atmosfera (IMPA) from Portugal, Instituto Geográfico Nacional (IGN) from Spain, and Real Observatorio de la Armada/Universidad Complutense de Madrid (ROA/UCM) from Spain (see Data and Resources),

The prototype configuration was performed using 84 representative earthquakes published in the IGN catalog that occurred between 2006 and 2011 (see Data and Resources), with moment magnitudes from 3.1 to 6.1 (Fig. 1). These earthquakes are clearly divided into two clusters: those located from 9° to 6° W were classified as GC earthquakes and those located from 11° to 9° W were classified as SV earthquakes.

Processing Module

The system configuration was optimized for detecting SV and GC earthquakes of interest, the locations of which showed the best compromise between accuracy and processing time for the available stations in the area.

After the real-time data acquisition, the processing chain, composed of the modules PICK_EEW, BINDER_EW, and EWPUBLISH, takes action. The module PICK_EEW comes

Table 1
Category, Main Functionality, and Source of the Earthquake Early Warning System (EEWS) Modules

Category	Module	Main Functionality	Source*
Processing	PICK_EEW	Picks waveforms and computes τ_c and P_d	A
	BINDER_EW	Event detection and location	O
	EWPUBLISH	M_w estimation from proxies	C
Archiving	WAVE_SERVERV	Temporary waveforms archive	O
	ORA_TRACE_SAVE	Saves waveforms into a database	M
	ORAREPORT	Saves event, including early warning data, into a database	M
Dissemination	EWSERVER	Disseminates event and early warning data	C
	EWMONITOR	Collects disseminated event and early warning data and computes lead times	C
Control	Control modules	State-of-health control	O

*O, original from Earthworm; M, slightly modified from the original Earthworm module; A, adapted; C, created from scratch.

from the module PICK_EW, an implementation of the short-term average/long-term average picking algorithm developed by Allen (1978). All the steps of the *P*-wave detection procedure are controlled by a set of parameters (Allen, 1978; Mele *et al.*, 2010) that require complex fine tuning for each station. Their optimization will reduce picking errors and the detections of false events, which has been experienced in the Automatic Determination System at ICGC.

The configuration was performed by simulating the behavior of the PICK_EEW module over the 427 vertical components of the mentioned offline data (Pazos *et al.*, 2015), after discarding EGOR and PVLZ stations due to the limited number of records (<3). For the rest of the 22 stations, the parameters (Mele *et al.*, 2010) were fine tuned to detect *P* waves (Table 2) with a maximum difference of 0.5 s with the actual arrival and in a very fast way (e.g., coda finalization parameter MinCodaLen was set to zero because it is time consuming).

Results obtained during the testing process are shown in Figure 3. The horizontal axis of the chart shows the difference, in seconds, between the automatic and real *P*-arrival times, and the vertical axis represents the number of occurrences. In order to figure out the general behavior of each station, the median of the differences (ΔTmedian) was calculated for each one. The results showed the stations could be classified in three different groups: reliable (ΔTmedian <0.1 s), acceptable (ΔTmedian between 0.1 and 0.2 s), and unreliable (ΔTmedian between 0.2 and 0.5 s).

Table 2
PICK_EEW Module Main Parameters for the *P*-Wave Automatic Detection

Parameter	Classification	Configured Value
Itr1	Trigger evaluation	3–15
MinSmallZC	Trigger finalization	30
MinBigZC	Trigger finalization	10–20
MinPeakSize	Trigger finalization	Depending on SNR
MaxMint	Trigger finalization	50
MinCodaLen	Trigger/coda finalization	0
CharFuncFIlt	Filtering	0.02
StaFilt	Filtering	0.2
LtaFilt	Filtering	0.000055
EventThresh	Filtering	10–45
RmavFilt	Filtering	0.9960
CodaTerm	Coda finalization	Depending on SNR
AltCoda	Coda finalization	1

SNR, signal-to-noise ratio.

It is also shown that the majority (79%) of the differences correspond to 0–0.3 s. Greater differences (>1 s) correspond to poor-quality records, and they make up only 5% of the differences, demonstrating the good accuracy of the automatic picking. The quality of the records is calculated offline as the ratio between a function of the waveform in the window where seismic signal is present (i.e., between the actual *P*-arrival time and the end of the coda) and the same function applied to a noise window (typically, from the beginning of the record until the actual *P*-arrival time). That function is computed as the squared amplitude of the samples of the waveform in counts, filtered with the same high-pass filter used in the automatic picking module, divided by the length of the windows where the function was applied.

A noticeable change of this module is the computation of the magnitude proxies P_d (peak displacement of the *P*-wave signal) and τ_c (predominant period of the *P*-wave signal). The first is defined as the peak displacement of the first few seconds of the *P*-wave signal, and τ_c is the predominant period of the *P*-wave signal originally defined by Kanamori (2005):

$$\tau_c = 2\pi\sqrt{\frac{\int_0^a u^2(t)\mathrm{d}t}{\int_0^a v^2(t)\mathrm{d}t}}, \tag{1}$$

in which a is equal to τ_0 and u and v are the ground displacement and velocity, respectively, both computed over a time window of duration τ_0 starting at the *P*-wave onset time. Because the procedure of the standard module PICK_EW is based on near-real-time operation, which means that each sample is processed sequentially, and a pick is detected at the same time that it happens (except for the latency; i.e., the delay introduced by the transmission), the program is not allowed to access earlier values unless they were previously stored in memory. In this way, the module was modified to continuously compute the velocity (removing the instrumental response) and the displacement (integrating the velocity) in real time. We also applied a high-pass infinite impulse response filter with a customizable corner frequency, typically 0.075 Hz (Wu *et al.*, 2007), to remove the low-frequency content.

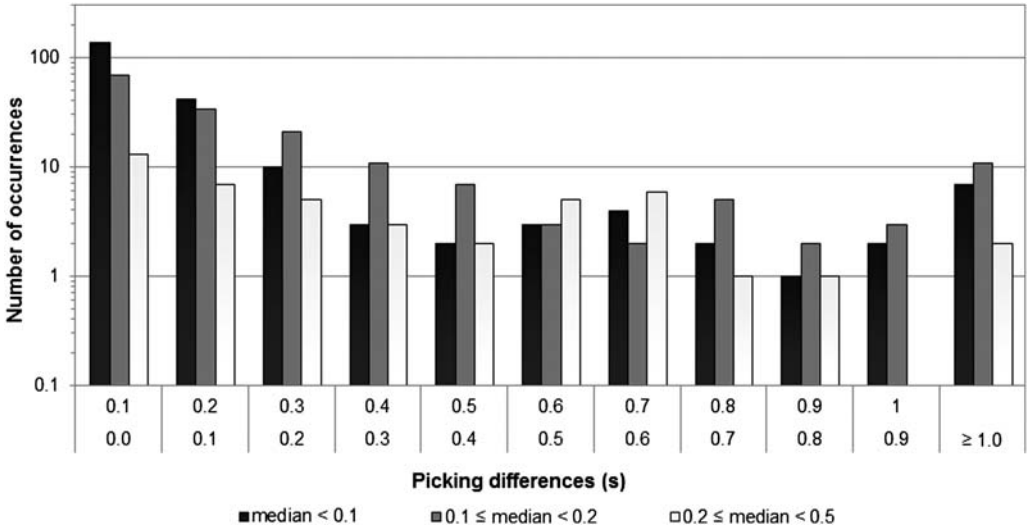

Figure 3. Distribution of the differences in the picks according to the median. The horizontal axis of the chart shows the difference, in seconds, between the automatic and real *P*-arrival times. The vertical axis shows the number of occurrences of three groups of stations: black, medians less than 0.1 s; gray, medians between 0.1 and 0.2 s; and white, medians between 0.2 and 0.5 s.

This procedure will allow the proxies to be calculated at the time of the onset of the pick. First, the displacement will be evaluated sample by sample to find its maximum (P_d) in a window of τ_0 s. At the end of the τ_0 window, τ_c will be calculated. Although the typical value of τ_0 in the literature is 3 s, Colombelli *et al.* (2012) showed that better magnitude estimates of very large earthquakes, associated with finite faults, could be obtained if the proxies were evaluated for longer τ_0 lengths up to the *S*-wave arrival time, in order to take into account secondary patches of the total rupture and not only a point-source hypothesis. Thus, the prototype implements several τ_0 windows, all of them starting at the onset of the pick with variable length from 3 s up to a limit of 15 s, in steps of 1 s. For every window, P_d and τ_c are computed, obtaining progressive updated values of the proxies. Because the *S-P* interval depends on the hypocentral distance, the maximum length of the τ_0 windows is variable, ensuring τ_0 windows end before the arrival of *S* waves and avoiding errors in τ_c and P_d computation. Our proposal is to use the running average of the absolute value (AAV), so τ_0 will extend up to the first local minimum of AAV or up to the theoretical arrival time of *S* waves is reached.

In addition, a signal-to-noise ratio (SNR) applied to the displacement signal was introduced to discard the P_d and τ_c proxies if the *P* wave is too weak. It was implemented through the continuous calculation of the signal power of the trace and the SNR computation at $\tau_0 = 3$ s. P_d and τ_c proxies computed from displacement waveforms with SNR lower than a configurable threshold are rejected.

Event Detection and Location

A stand-alone BINDER_EW, called SimBinder, was developed to study offline the complexity of the Earthworm module. Thanks to simulations of earthquakes of interest (Pazos *et al.*, 2015) (Fig. 1), the different configurable parameters were tuned to adapt the prototype BINDER_EW module for EEW purposes by simplifying its procedures into two steps: the stacking and the new phase association process.

The goal of the stacking process is the event declaration, which is triggered by a successful intersection of the hyperboloids built from the picking of the first arrivals. This intersection is used as a seed to an iterative locator to obtain a final location. The key parameters of this first step are the grid specification and the number of picks needed for the declaration.

SimBinder simulations (Pazos *et al.*, 2015) and historical seismicity constrained the study grid (35°–37° N, 11°–6° W), the area where the detected SV and GC earthquakes were expected to be located. The evaluation of benefits of event location quality and the time required to detect the event by at least four stations (the minimum number required by the system to locate an event) was also carried out using simulations. Results for the M_w 5.5 SV earthquake on 17 December 2009 are shown in Figure 4. The vertical axes of the charts show the differences in origin time (seconds) and distance between epicenters (kilometers) between the automatically determined and IGN locations, and the horizontal axes show the elapsed time from the origin time. Distances between locations are shown from the creation of the event to the last location update. Forty-two seconds after the earthquake occurs (Fig. 4), the system is able to provide a first location with an error of approximately 75 km (from four stations). Only 5 s later, the obtained locations are very reliable with errors of only 5 km and only 1 s in origin time (from six stations). The figure also shows the progression of the differences for each updated location. These results are representative of all the simulations and demonstrate that the module BINDER_EW configured as a six-station system is a suitable compromise between precision and elapsed time.

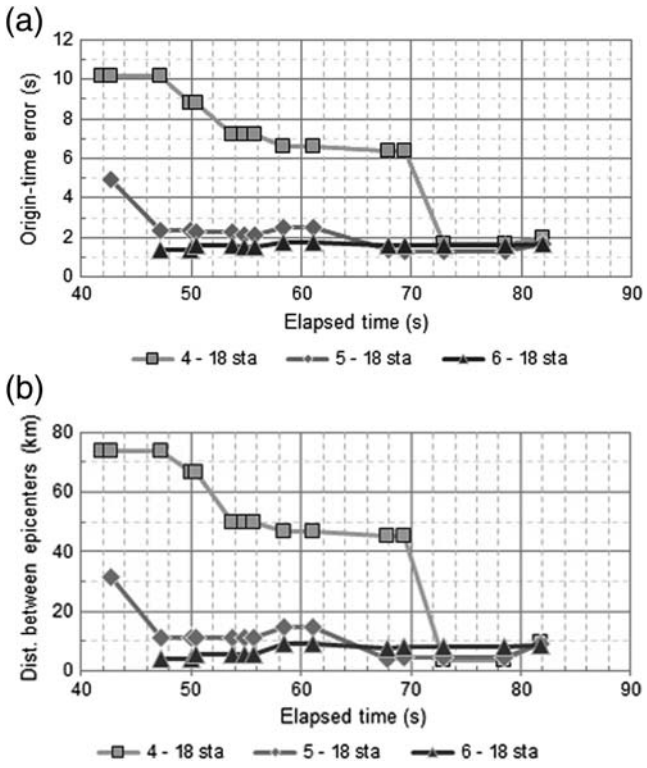

Figure 4. Differences in (a) the origin time and (b) distances between epicenters, comparing the automatically determined ones with IGN locations for the M_w 5.5 SV earthquake on 17 December 2009, versus the elapsed time from the origin time (in seconds). Lines with square symbols show the progression of the differences for an event created from four phases, lines with rhomboid symbols show the progression that starts with five phases, and lines with triangular symbols show the progression that starts with six phases. Each square, rhomboid, or triangle indicates a new update that takes into account information from a new pick.

The second step of the prototype BINDER_EW refers to the association of new pick arrivals to the currently active event. This association is driven by three constraints, based on time, space, and the tolerance of the difference between observed and calculated arrival times (O-C residuals) resulting from the combination of multiple parameters. Time and space based parameters were tuned by taking into account communication latencies and the area extension, respectively. The final decision for a new association and a new relocation depends on the calculated O-C residual tolerance, which depends on several factors: number of pickings, root mean square, and the epicentral distance of the new station. The parameters controlling the last constraint were empirically tuned in order to only accept coherent phases for smaller distances and increase tolerance as epicentral distance increases.

Magnitude Estimation

The module EWPUBLISH was created especially for this prototype to assemble all the information that was received from the two preceding processing modules, PICK_EEW and BINDER_EW, and to build a standard Earthworm message for every declared event. It receives location messages from the BINDER_EW, plus several messages from PICK_EEW (which contain all the picks used to locate it), and computes its residuals, and epicentral and hypocentral distances. It also receives all the P_d and τ_c proxies computed from channels of the picks used for the event location. Because several values of τ_0 are possible for each pick, the values of the proxies are continuously updated. Thus, the magnitude will be estimated under certain configurable constraints: the P_d values must be greater than 10^{-5} cm, the epicentral distance must be less than 300 km, and τ_0 must be less than the estimated difference between the arrival times of the *S* and *P* waves, guaranteeing that τ_0 will end before the *S* arrival even at very short epicentral distances.

If all these constraints are overcome, the estimates of the moment magnitude through the proxies are made as described by Carranza (2012) and Carranza *et al.* (2013): on one hand, equation (2) relates the peak displacement (P_d in centimeters), normalized to a reference distance of 200 km, with M_{wP_d}:

$$\log_{10}|P_{d200}| = 1.0M_{wP_d} - 8.3. \quad (2)$$

The normalization of P_d is expressed as a function of the hypocentral distance (R in km) in the following formula:

$$P_{d200} = P_d \times 10^{-1.7\times\log 10|\frac{200}{R}|}. \quad (3)$$

On the other hand, equation (4) relates the parameter τ_c as a function of the moment magnitude $M_{w\tau_c}$:

$$\log_{10}|\tau_c| = 0.3M_{w\tau_c} - 1.6. \quad (4)$$

The magnitude estimated by the module will be based on the linear combination (equation 5) of the estimates M_{wP_d} and $M_{w\tau_c}$ and will be calculated as the median of the magnitudes from each channel:

$$M_w = \alpha M_{wP_d} + \beta M_{w\tau_c}, \quad (5)$$

in which $\alpha + \beta = 1; 0 \le \alpha \le 1; 0 \le \beta \le 1$.

The final magnitude will be computed only over the channels with significant *P*-wave amplitude that exceed a threshold on the SNR calculated over the displacement signal. That threshold was empirically set to 9, taking into account several earthquakes with magnitudes over 3.5.

Data Archiving and EEW Dissemination

Parallel to the processing tasks (Fig. 2), the event data and waveforms are saved into the database designed for this purpose. To adapt archiving modules to this database, ORA_TRACE_SAVE and ORAREPORT modules have been slightly modified.

Whereas the objective of any EEWS is to provide rapid notification of the potential damaging effects at specific targets of an impending earthquake with enough time to react, EWSERVER and EWMONITOR modules were developed for EEW dissemination. Multiple EWMONITOR modules

can operate simultaneously at different locations, with customized configurations, connected to EWSERVER via a Transmission Control Protocol/Internet Protocol (TCP/IP) socket connection, receiving data of detected and located earthquakes and creating EEW messages.

Real-Time Operation

The described EEWS based on Earthworm tools was developed and installed using the existing real-time seismic stations available at the region. The Data Reception Center, located at ICGC in Barcelona, receives continuous real-time seismic data from the 24 broadband stations in the area (Fig. 1).

After the setting-up stage, a year of continuous real-time testing (from 23 July 2013 to 23 July 2014) with any station or configuration modifications was carried out. The main objective of the first year of continuous testing was to study the prototype behavior and performance for earthquakes of interest: those felt in the Iberian Peninsula and with $M_w > 4.0$ that occurred in the two clusters of SV and GC.

Real-Time Seismic Network

After the configuration and evaluation of the 24 broadband stations in the area (Fig. 1), a selection of the best-quality stations was used for the prototype. These stations are depicted in Figure 1 based on their reliability, depending on the picking error medians (always < 0.5 s) and the availability of high SNR records (at least 10) to configure them in the PICK_EEW module. Except for two stations depicted as white triangles (EGOR and PVLZ), all the available ones have been taken into account. Configured stations with low picking error median (< 0.2 s) and checked with 10–37 records are depicted as black triangles, and gray triangles indicate stations that are being tested because of their higher picking error medians (between 0.2 and 0.5 s) or their lack of enough records to check the configuration (Fig. 1).

The poor azimuthal coverage of stations (gap about 180°) is noticeable from Figure 1, especially for the SV earthquakes (gap about 270°). In addition, Moroccan stations (AVE and IFR) are too distant to be associated with the first location of most of the events, increasing the coverage gaps for first locations.

Results

During the real-time test period, only one earthquake of interest occurred. The GC earthquake of 16 December 2013 at 07:06:23 UTC with M_w 4.8 was felt with a European Macroseismic Scale 1998 (EMS-98) intensity of II in the Spanish coastal zone and III/IV in Portugal.

In order to evaluate the quality of the earthquake location, the location error was calculated in respect to the IGN catalog. The IGN catalog (see Data and Resources) was used as the reference because their locations are revised by an operator, who manually picks *P*- and *S*-wave arrivals and locates the events using the IGN velocity model, which is also used in our prototype. Events in the IGN catalog are located with the records from all the available stations of the IGN network, including the Canary Islands stations, as well as those that belong to other seismic networks, both in real time or on-demand transmission.

The GC earthquake of 16 December 2013 had fairly good results; the calculation of the prototype origin time is nearly 1 s later, and the event location is 9 km to the north-northwest of the IGN location. The automatic hypocenter was calculated at a depth of 63 km, differing by 23 km from the IGN catalog (40 km).

In contrast to records with weak *P*-wave signal SNR (such as in Fig. 5a), five of the six first displacement records of the GC earthquake of 16 December 2013 exceeded the SNR threshold (set to nine) (Fig. 5b). P_d and τ_c proxies were available for different τ_0 intervals in five channels (ECEU, CEU, PVAQ, EMIJ, and EGRO). Particularly, the evolution of τ_c proxy is shown in Figure 6.

Finally, moment magnitude was estimated using the empirical relationships proposed by Carranza *et al.* (2013) for this region and the P_d and τ_c proxies for the longest τ_0 intervals available at the time that the first complete solution was published. The median magnitude estimated from the P_d proxy of each channel was M_{wP_d} 4.96, whereas the median magnitude estimated from the τ_c proxies was $M_{w\tau_c}$ 3.95, giving a final averaged magnitude of 4.46, which is close to the 4.8 value from the IGN catalog as well as being a candidate earthquake to generate an alert.

False Alerts

Reliability as well as effectiveness is required for an EEWS; that is, the possibility of false alerts must be studied and minimized.

During the period test, a total of 56 SV and GC earthquakes with $M_w < 4.0$ were located in the zone of interest (35°–37° N, 11°–6° W), and another 42 earthquakes with M_w 1.8–4.9 and belonging to the surrounding area of the grid were detected. No other events (such as noise, teleseisms, or artificial explosions) were detected.

Nevertheless, none of the displacement records of these 98 events reached the SNR threshold over the displacement signal (set to 9); and, therefore, no magnitude estimation was carried out, reducing the detection of false alert to 0% during the test period.

EEW Monitoring

As an earlier step to producing a complete scenario with lead times and potential damages, we define a location scenario as a plot of the blind zone and the lead times to specific targets. These data are computed by means of the location and the warning time (i.e., the interval, in seconds, from the earthquake occurrence to the first alert generation). Warning time is computed by subtracting the automatic origin time from the time when the location scenario is published.

The processing chain results (picking, detection, location, and magnitude assessment) and the consequent blind zone and lead times values at targets are continuously computed and monitored in real time by the module EWMONITOR. Figure 7

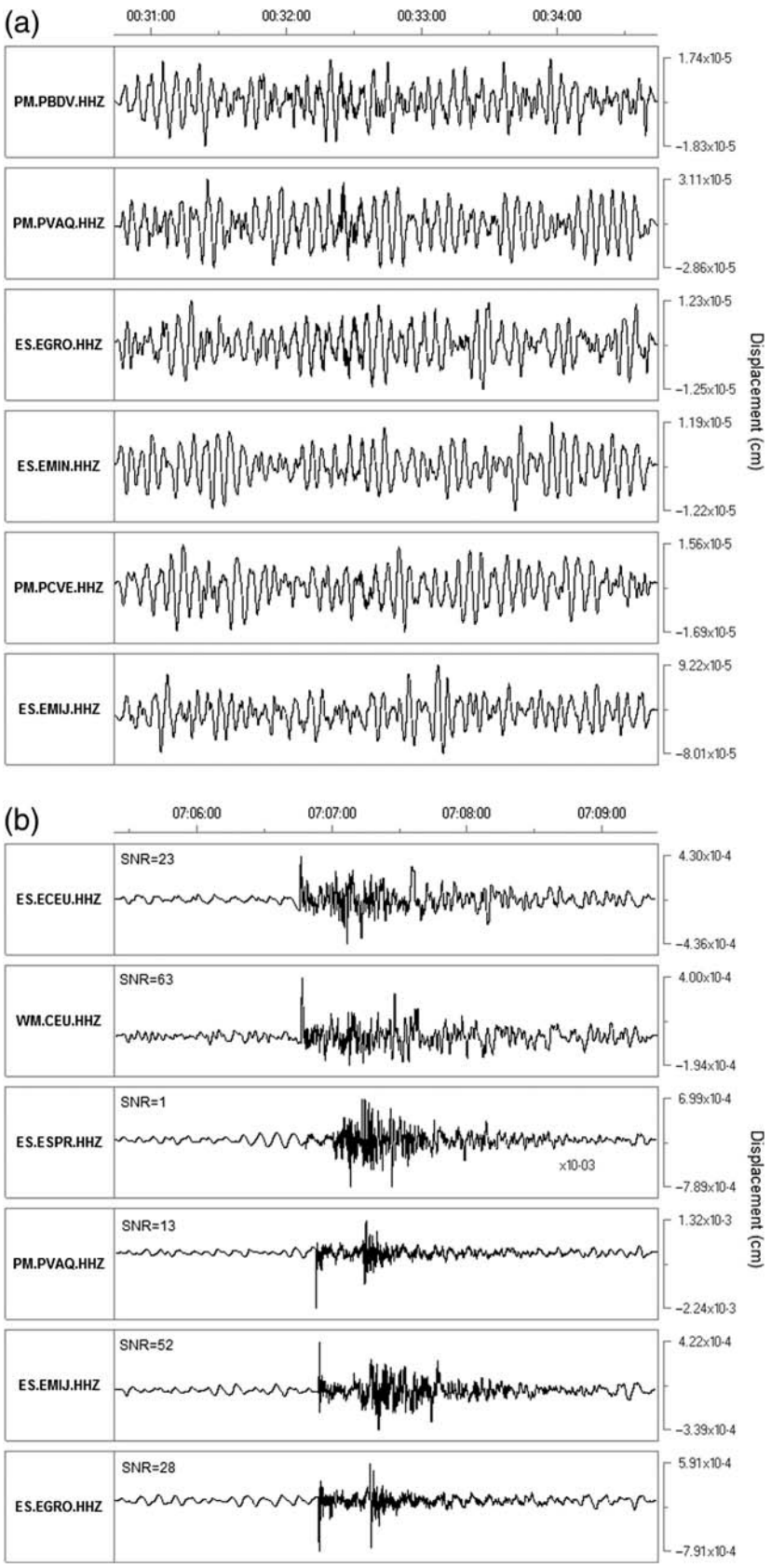

Figure 5. Displacement signals, in centimeters, at recording stations resulting from a high-pass Butterworth filter of two poles and a corner frequency of 0.075 Hz: (a) GC 24 July 2013 00:31:36 UTC M_w 3.8, and (b) GC 16 December 2013 07:06:23 UTC M_w 4.8.

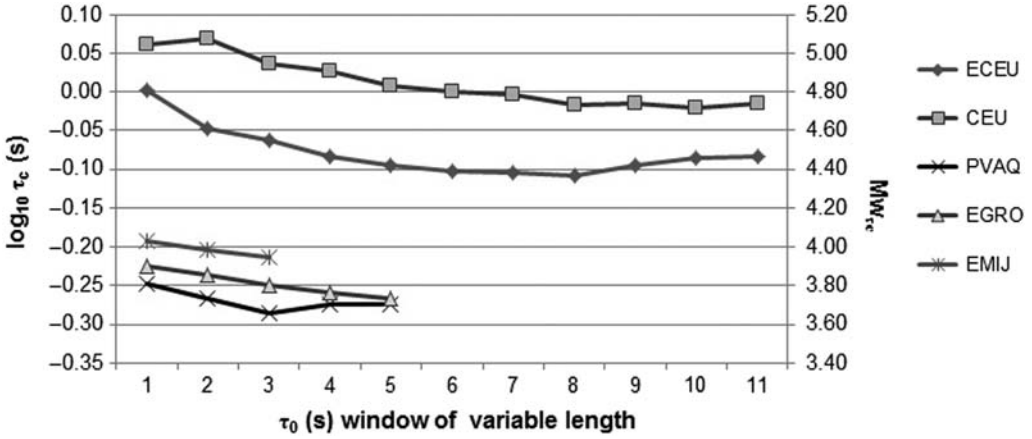

Figure 6. Evolution of the τ_c proxy for 16 December 2013 earthquake as a function of the τ_0 window for each channel (ECEU, CEU, PVAQ, EGRO, EMIJ) of the phases used to locate the event.

shows a screenshot of the EWMONITOR at the time when a first alert emission could have been generated for the GC earthquake of 16 December 2013. This screenshot belongs to the location scenario built by the prototype.

A warning time of 42 s is required to announce the occurrence of this GC earthquake (Fig. 7). This time increases by 1 s if the actual origin time is taken into account. The resulting warning time is composed of three terms: *P*-wave travel time from source to the sixth closest seismic station, data latency, and processing time. Data latency is related to the data acquisition and communication system; and, for the current deployment the mean value is 8.5 ± 2.5 s. However, processing time is only related to the architecture of the prototype and, for this case study, is 4 s. Finally, the *P*-wave travel time varies, depending on the distance between the source and the sixth closest seismic station, and it is the main contributor to the resulting warning time due to the long distance from stations to the two clusters. Installing new seismic stations closer to both clusters would reduce significantly the warning time and therefore increase available lead times.

Lead times to selected targets of the western and southern coast of Portugal and south of Spain are computed assuming an average *S*-wave velocity in the crust of 3.4 km/s. The automatic lead times at the main targets are large enough to be considered for producing alert for damage mitigation (10 s for Huelva, 19 s for Seville, 21 s for Portimão, 9 s for Faro, 72 s for Lisbon, and 49 s for Sines). Unfortunately, on the Spanish coast, Cádiz has a lead time of −8 s.

Comparing these values to the actual lead times, all of them increase between 1 and 2 s, with the actual situation being more optimistic than the prototype interpretation. These results are consistent with the fact that the automatic epicenter is located slightly closer to the seismic net because of its lack of azimuthal coverage.

Conclusions

A prototype of the regional EEWS for southwest Iberia was designed with modules that are available in Earthworm tools. Several of those modules were modified and others were created to meet the requirements of an EEWS, particularly the computation of the proxies and magnitude assessment with a minimum delay.

The system has five different module functionalities: data acquisition, processing, data archiving, EEW dissemination, and state-of-health control. Its design is focused on the processing modules to be able to optimize the time to obtain a first location and estimated M_w of an acceptable quality. Once the system has achieved these results, an alert emission could take place. At present, to complete the system with potential damage zones estimations, existing ground motion and intensity prediction equations are being examined to select the most adequate equations fitting local strong motion and intensity data.

This system works with the real-time seismic stations available in the region. After the configuration stage, low picking errors (0.3 s in 79% of the 427 simulations) are obtained for a group of 17 stations, 5 stations are still under test, and 2 were discarded because of higher picking errors. An SNR threshold value of 9 applied to the displacement signals was established in order to avoid P_d and τ_c proxies and M_w estimates from low-magnitude events or records with *P* waves that are too weak.

In a previous study (Pazos *et al.*, 2015), offline results showed that using a minimum of six stations to identify an event provides the best compromise between the precision of the hypocentral parameters and the elapsed time for the present distribution of the stations in the network.

During a one-year test period in real time, an earthquake of interest occurred; it was successfully detected by the prototype and identified as a candidate for alert emission. A comparison between the actual hypocentral parameters determined by IGN and the parameters detected by the EEW shows that the result for the GC earthquake of 16 December 2013 M_w 4.8 is fairly good in both the origin time difference (nearly 1 s) and the distance between the epicenters (9 km to the north-northwest). Furthermore, this earthquake also had acceptable

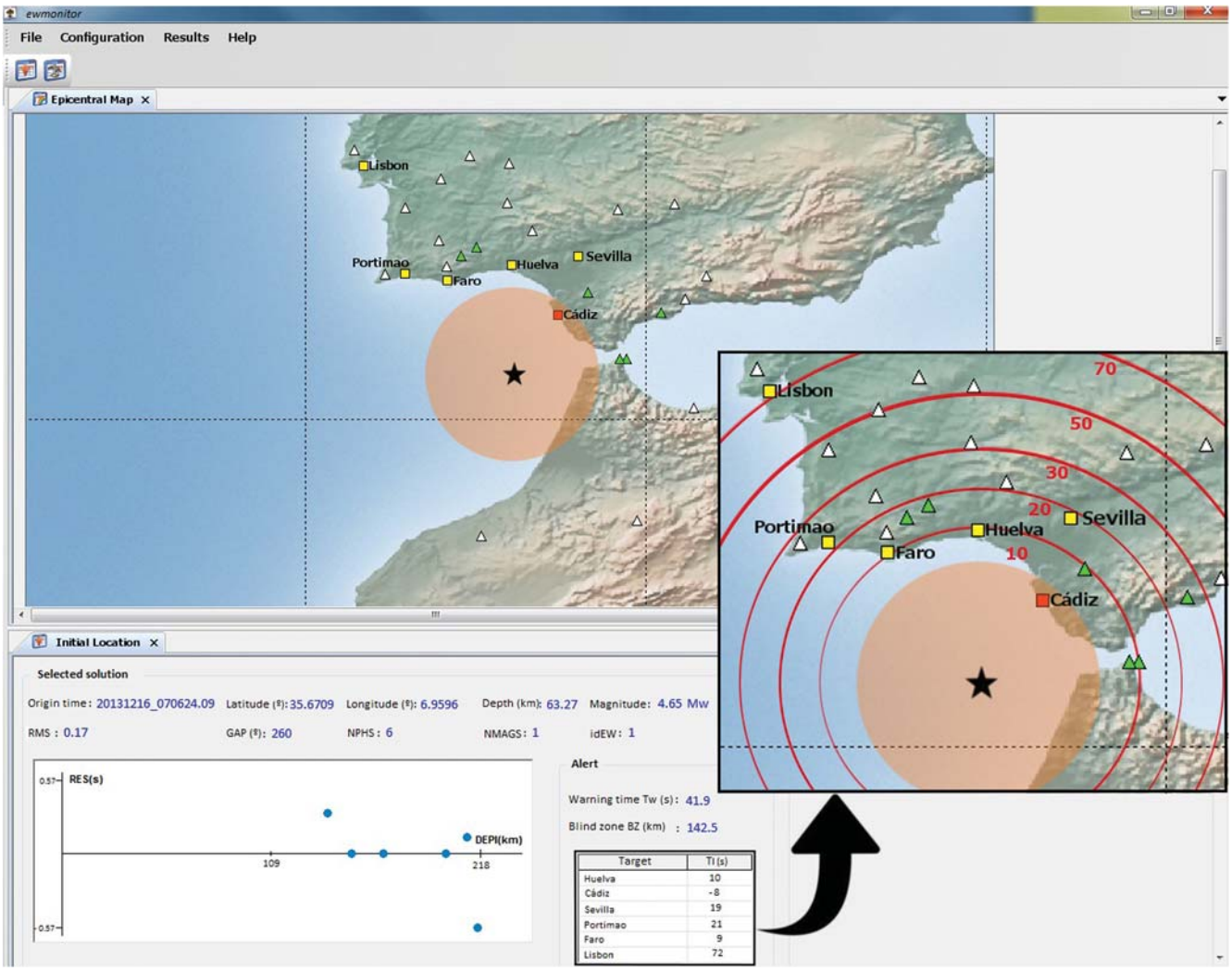

Figure 7. The EWMONITOR module for the GC earthquake of 16 December 2013: star, first automatic epicenter location ; orange-filled circle, blind zone; white and green triangles, not-triggered and triggered stations, respectively; red and yellow squares, targets inside the blind zone and targets with positive lead times, respectively; and numerical results. In the enlarged map, resulting lead times are represented by red circles, centered on the epicenter, at the time the warning message is received by EWMONITOR.

displacement signal results, and the moment magnitude estimate was 4.46, similar to the IGN catalog value.

Considering reliability, another 98 events corresponding to the SV and GC clusters and its surrounding areas were detected during the test period. Nevertheless, because none of these earthquakes exceeded the SNR displacement threshold of 9 and none were felt in Iberia, requirements for alert emission were not accomplished, and no false alerts took place.

Regarding effectiveness, for the single detection of interest, the prototype was ready for alert emission 42 s after the automatic earthquake occurrence. The majority of southwest Iberian targets, such as Huelva and Seville in Spain and Portimão, Faro, and Sines in Portugal, had automatic lead time values large enough to be considered for damage mitigation (between 10 and 49 s). Nevertheless, the lead time for Cádiz (−8 s) shows that is within the blind zone. Taking into account the IGN location, these results only differ between 1 and 3 s and demonstrate the feasibility of this prototype EEWS for the southwest Iberian Peninsula except for some coastal areas.

To sum up, for a first-year period test, prototype behavior and performance in real time is satisfactory even with azimuthal coverage disadvantages, although a longer test period is needed to confirm the accuracy of the prototype for the earthquakes of interest.

Data and Resources

Records used in this study were collected from the three broadband seismic networks: Instituto Português do Mar e da Atmosfera (IMPA) (for more information contact info@ipma.pt) from Portugal, and Western Mediterranean (for more information contact webmaster@roa.es) and Instituto Geográfico Nacional (IGN) (for more information contact sismologia@fomento.es) from Spain. Access to the waveform records can be obtained from the owners on request. The cata-

log used as reference for reliability and effectiveness determination of the system is from IGN (http://www.ign.es/ign/layoutIn/sismoFormularioCatalogo.do, last accessed October 2014).

Acknowledgments

This work was partially funded by the Spanish ALERT-ES (CGL2010-19803-C03) and ALERTES RIM (CGL2013-45724-C3-2-R) projects. We thank Real Instituto y Observatorio de la Armada in San Fernando, and especially Antonio Pazos and Javier Gallego, for creating the database of earthquakes in the study area and for providing the real-time data at Institut Cartogràfic i Geològic de Catalunya. We want to thank Aldo Zollo for fruitful discussions during the ALERT-ES meetings. Also, we thank the Western Mediterranean, Instituto Português do Mar e da Atmosfera, and Instituto Geográfico Nacional networks for making their data available. Finally, we are very grateful to Da-Yi Chen and to an anonymous reviewer whose comments greatly improved the quality of the article.

References

Alcik, H., O. Ozel, N. Apaydin, and M. Erdik (2009). A study on warning algorithms for Istanbul earthquake early warning system, *Geophys. Res. Lett.* **36,** L00B05, doi: 10.1029/2008GL036659.

Allen, R. M., and H. Kanamori (2003). The potential for earthquake early warning in southern California, *Science* **300,** 786–789.

Allen, R. M., H. Brown, M. Hellweg, O. Khainovski, P. Lombard, and D. Neuhauser (2009). Real-time earthquake detection and hazard assessment by ElarmS across California, *Geophys. Res. Lett.* **36,** L00B08, doi: 10.1029/2008GL036766.

Allen, R. V. (1978). Automatic earthquake recognition and timing from single traces, *Bull. Seismol. Soc. Am.* **68,** no. 5, 1521–1532.

Baptista, M. A., P. M. A. Miranda, F. Chierici, and N. Zitellini (2003). New study of the 1755 earthquake source based on multi-channel seismic survey data and tsunami modeling, *Nat. Hazards Earth Syst. Sci.* **3,** 333–340.

Böse, M., E. Hauksson, K. Solanki, H. Kanamori, and T. H. Heaton (2009). Real-time testing of the on-site warning algorithm in southern California and its performance during the July 29, 2008 M_w 5.4 Chino Hills earthquake, *Geophys. Res. Lett.* **36,** L00B03, doi: 10.1029/2008GL036366.

Böse, M., C. Ionescu, and F. Wenzel (2007). Earthquake early warning for Bucharest, Romania: Novel and revisited scaling relations, *Geophys. Res. Lett.* **34,** L07302, doi: 10.1029/2007GL029396.

Böse, M., F. Wenzel, and M. Erdik (2008). PreSEIS: A neural networkbased approach to earthquake early warning for finite faults, *Bull. Seismol. Soc. Am.* **98,** no. 1, 366–382, doi: 10.1785/0120070002.

Brown, H., R. M. Allen, and V. F. Grasso (2009). Testing ElarmS in Japan, *Seismol. Res. Lett.* **80,** no. 5, 727–739, doi: 10.1785/gssrl.80.5.727.

Buforn, E., M. Bezzeghoud, A. Udías, and C. Pro (2004). Seismic sources on the Iberia-African plate boundary and their tectonic implications, *Pure Appl. Geophys.* **161,** 623–646.

Buforn, E., A. Udías, and J. Mezcua (1988). Seismicity and focal mechanism in south Spain, *Bull. Seismol. Soc. Am.* **78,** 2008–2024.

Carranza, M. (2012). Obtención de parámetros P_d y τ_c para el SW de Iberia, *Master degree final project*, Universidad Complutense de Madrid, Spain (in Spanish)

Carranza, M., E. Buforn, S. Colombelli, and A. Zollo (2013). Earthquake early warning for southern Iberia: A *P* wave threshold-based approach, *Geophys. Res. Lett.* **40,** no. 17, 4588–4593, doi: 10.1002/grl.50903.

Chen, D. Y., N. C. Hsiao, and Y. M. Wu (2015). The Earthworm-based earthquake alarm reporting system in Taiwan, *Bull. Seismol. Soc. Am.* **105,** 568–579.

Chen, W. P., and N. Grimison (1989). Earthquakes associated with diffuse zones of deformation in the oceanic lithosphere: Some examples, *Tectonophysics* **418,** 277–297.

Colombelli, S., A. Zollo, G. Festa, and H. Kanamori (2012). Early magnitude and potential damage zone estimates for the great M_w 9 Tohoku-Oki earthquake, *Geophys. Res. Lett.* **39,** L22306, doi: 10.1029/2012GL053923.

Cua, G., and T. Heaton (2007). The Virtual Seismologist (VS) method: A Bayesian approach to earthquake early warning, in *Earthquake Early Warning Systems*, P. Gasparini, G. Manfredi, and J. Zschau (Editors), Springer, Heidelberg, Germany, 97–132.

Erdik, M., Y. Fahjan, O. Ozel, H. Alcik, A. Mert, and M. Gul (2003). Istanbul earthquake rapid response and the early warning system, *Bull. Earthq. Eng.* **1,** 157–163.

Espinosa-Aranda, J. M., A. Cuellar, A. Garcia, G. Ibarrola, R. Islas, S. Maldonado, and F. H. Rodriguez (2009). Evolution of the Mexican Seismic Alert System (SASMEX), *Seismol. Res. Lett.* **80,** no. 5, 694–706, doi: 10.1785/gssrl.80.5.694.

Espinosa-Aranda, J. M., A. Jimenez, G. Ibarrola, F. Alcantar, A. Aguilar, M. Inostroza, and S. Maldonado (1995). Mexico City Seismic Alert System, *Seismol. Res. Lett.* **66,** no. 6, 42–53.

Goula, X., P. Dominique, B. Colas, J. A. Jara, A. Roca, and T. Winter (2008). Seismic rapid response system in the eastern Pyrenees, *XIV World Conference on Earthquake Engineering*, Beijing, China, 12–17 October 2008

Goula, X., J. A. Jara, T. Susagna, and A. Roca (2001). A new broad-band seismic network with satellite transmission in Catalonia (Spain), *ORFEUS Newsletter* **3,** no. 1, http://www.orfeus-eu.org/organization/Organization/Newsletter/vol3no1/catalonianet.html (last accessed November 2015).

Gràcia, E., J. Dañobeitia, J. Vergés, R. Bartolomé, and D. Córdoba (2003). Crustal architecture and tectonic evolution of the Gulf of Cadiz (SW Iberian margin) at the convergence of the Eurasian and African plates, *Tectonics* **22,** no. 4, doi: 10.1029/2001TC901045.

Grandin, R., J. F. Borges, M. Bezzegoud, B. Caldeira, and F. Carrilho (2007). Simulations of strong ground motion in SW Iberia for the 1969 February 28 (M_s 8.0) and the 1755 November 1 (M 8.5) earthquakes—II. Strong ground motion simulations, *Geophys. J. Int.* **171,** no. 2, 807–822, doi: 10.1111/j.1365-246X.2007.03571.x.

Grimison, N., and W. Chen (1986). The Azores—Gibraltar plate boundary: Focal mechanisms, depth of earthquakes and their tectonic implications, *J. Geophys. Res.* **91,** no. B2, 2029–2047, doi: 10.1029/JB091iB02p02029.

Gutscher, M.-A., M. A. Baptista, and J. M. Miranda (2006). The Gibraltar arc seismogenic zone (Part 2): Constraints on a shallow east dipping fault plane source for the 1755 Lisbon earthquake provided by tsunami modeling and seismic intensity, *Tectonophysics* **426,** nos. 1/2, 153–166, doi: 10.1016/j.tecto.2006.02.025.

Horiuchi, N. J., S. H. Negishi, K. Abe, A. Kamimura, and Y. Fujinawa (2005). An automatic processing system for broadcasting earthquake alarms, *Bull. Seismol. Soc. Am.* **95,** 708–718.

Hoshiba, M., O. Kamigaichi, M. Saito, S. Tsukada, and N. Hamada (2008). Earthquake early warning starts nationwide in Japan, *Eos Trans. AGU* **89,** no. 8, 73–74.

Hsiao, N.-C., Y.-M. Wu, T.-C. Shin, L. Zhao, and T.-L. Teng (2009). Development of earthquake early warning system in Taiwan, *Geophys. Res. Lett.* **36,** L00B02, doi: 10.1029/2008GL036596.

Ionescu, C., M. Böse, F. Wenzel, A. Marmureanu, A. Grigore, and G. Marmureanu (2007). Early warning system for deep Vrancea (Romania) earthquakes, in *Earthquake Early Warning Systems*, P. Gasparini, G. Manfredi, and J. Zschau (Editors), Springer, Heidelberg, Germany, 343–349.

Johnson, C. E., A. Bittenbinder, B. Bogaert, L. Dietz, and W. Kohler (1995). Earthworm: A flexible approach to seismic network processing, *IRIS Newsletter* **14,** 4.

Kamigaichi, O., M. Saito, K. Doi, T. Matsumori, S. Tsukada, K. Takeda, T. Shimoyama, K. Nakamura, M. Kiyomoto, and Y. Watanabe (2009). Earthquake early warning in Japan: Warning the general public and future prospects, *Seismol. Res. Lett.* **80,** no. 5, 717–726.

Kanamori, H. (2005). Real-time seismology and earthquake damage mitigation, *Annu. Rev. Earth Planet. Sci.* **33,** 195–214, doi: 10.1146/annurev.earth.33.092203.122626.

Köhler, N., G. Cua, F. Wenzel, and M. Böse (2009). Rapid source parameter estimations of southern California earthquakes using PreSEIS, *Seismol. Res. Lett.* **80,** no. 5, 748–754.

Mele, F., A. Bono, V. Lauciani, A. Mandiello, C. Marcocci, S. Pintore, M. Quintiliani, L. Scognamiglio, and S. Massa (2010). Tuning an Earthworm phase picker: Some considerations on the PICK_EW parameters, *INGV Technical Report 164*, 6–18.

Nakamura, Y. (1984). Development of earthquake early-warning system for the Shinkansen, some recent earthquake engineering research and practical in Japan, *Proc. of The Japanese National Committee of the International Association for Earthquake Engineering*, Tokyo, Japan, 224–238.

Nakamura, Y. (1988). On the urgent earthquake detection and alarm system (UrEDAS), *Proc. of the 9th World Conference on Earthquake Engineering*, Tokyo-Kyoto, Japan, 2–9 August 1988, 673–678.

Nakamura, Y., and J. Saita (2007). UrEDAS, the earthquake warning system: Today and tomorrow, in *Earthquake Early Warning Systems*, P. Gasparini, G. Manfredi, and J. Zschau (Editors), Chapter 13, Springer, New York, New York, 249–282.

Odaka, T., K. Ashiya, S. Tsukada, S. Sato, K. Ohtake, and D. Nozaka (2003). A new method of quickly estimating epicentral distance and magnitude from a single seismic record, *Bull. Seismol. Soc. Am.* **93,** 526–532.

Olivieri, M., and J. Clinton (2012). An almost fair comparison between Earthworm and SeisComP3, *Seismol. Res. Lett.* **83,** no. 4, 720–727, doi: 10.1785/0220110111.

Pazos, A., N. Romeu, L. Lozano, Y. Colom, M. López Mesa, X. Goula, J. A. Jara, and J. V. Cantavella (2015). A regional approach for earthquake early warning in southwest Iberia: A feasibility study, *Bull. Seismol. Soc. Am.* **105,** no. 2A, 560–567, doi: 10.1785/0120140101.

Peng, H. S., Z. L. Wu, Y. M. Wu, S. M. Yu, D. N. Zhang, and W. H. Huang (2011). Developing a prototype earthquake early warning system in the Beijing capital region, *Seismol. Res. Lett.* **82,** 394–403.

Romeu, N., J. A. Jara, X. Goula, T. Susagna, S. Figueras, C. Olivera, and A. Roca (2006). Sistema automático de información sísmica, in *5th Asamblea Hispano-Portuguesa de Geodesia y Geofísica*, Seville, Spain, 30 January–3 February 2006 (in Spanish).

Satriano, C., Y.-M. Wu, A. Zollo, and H. Kanamori (2011). Earthquake early warning: Concepts, methods and physical grounds, *Soil Dynam. Earthq. Eng.* **31,** 106–118, doi: 10.1016/j.soildyn.2010.07.007.

Shieh, J. T., Y.-M. Wu, and R. M. Allen (2008). A comparison of τ_c and τ_p^{max} for magnitude estimation in earthquake early warning, *Geophys. Res. Lett.* **35,** L20301, doi: 10.1029/2008GL035611.

Udias, A., and A. López-Arroyo (1970). Body and surface wave study of source parameters of the March 15, 1964 Spanish earthquake, *Tectonophysics* **9,** 323–346.

Wenzel, F., M. Onescu, M. Baur, and F. Fiedrich (1999). An early warning system for Bucharest, *Seismol. Res. Lett.* **70,** 161–169.

Wu, Y.-M., and H. Kanamori (2005a). Experiment on an onsite early warning method for the Taiwan early warning system, *Bull. Seismol. Soc. Am.* **95,** 347–353.

Wu, Y.-M., and H. Kanamori (2005b). Rapid assessment of damage potential of earthquakes in Taiwan from the beginning of P waves, *Bull. Seismol. Soc. Am.* **95,** 1181–1185.

Wu, Y.-M., and H. Kanamori (2008a). Development of an earthquake early warning system using real-time strong motion signals, *Sensors* **8,** 1–9.

Wu, Y.-M., and H. Kanamori (2008b). Exploring the feasibility of onsite earthquake early warning using close-in records of the 2007 Noto Hanto earthquake, *Earth Planets Space* **60,** 155–160.

Wu, Y.-M., and T.-L. Teng (2002). A virtual subnetwork approach to earthquake early warning, *Bull. Seismol. Soc. Am.* **92,** 2008–2018.

Wu, Y.-M., and L. Zhao (2006). Magnitude estimation using the first three seconds *P*-wave amplitude in earthquake early warning, *Geophys. Res. Lett.* **33,** L16312, doi: 10.1029/2006GL026871.

Wu, Y.-M., H. Kanamori, R. Allen, and E. Hauksson (2007). Determination of earthquake early warning parameters, τ_c and P_d, for southern California, *Geophys. J. Int.* **170,** 711–717, doi: 10.1111/j.1365-246X.2007.03430.x.

Wu, Y.-M., H.-Y. Yen, L. Zhao, B.-S. Huan, and W.-T. Liang (2006). Magnitude determination using initial *P* waves: A single station approach, *Geophys. Res. Lett.* **33,** L05306, doi: 10.1029/2005GL025395.

Yamada, M., and T. Heaton (2008). Real-time estimation of fault rupture extent using envelopes of acceleration, *Bull. Seismol. Soc. Am.* **98,** 607–619.

Zollo, A., G. Iannaccone, V. Convertito, L. Elia, I. Iervollino, M. Lancieri, A. Lomax, C. Martino, C. Satriano, E. Weber, *et al.* (2009). The earthquake early warning system in southern Italy, in *Encyclopedia of Complexity and System Science*, Vol. 5, 2395–2421, doi: 10.1007/978-0-387-30440-3.

Zollo, A., G. Iannaccone, M. Lancieri, V. Convertito, A. Emolo, G. Festa, F. Gallovic, M. Vassallo, C. Martino, C. Satriano, *et al.* (2009). Earthquake early warning system in southern Italy: Methodologies and performance evaluation, *Geophys. Res. Lett.* **36,** L00B07, doi: 10.1029/2008GL036689.

Zollo, A., M. Lancieri, and S. Nielsen (2006). Earthquake magnitude estimation from peak amplitudes of very early seismic signals on strong motion records, *Geophys. Res. Lett.* **33,** L23312, doi: 10.1029/2006GL027795.

Institut Cartogràfic i Geològic de Catalunya
Parc de Montjuïc
08038 Catalonia, Barcelona
Spain
nuria.romeu@icgc.cat
yolandacolom@gmail.com
joseantonio.jara@icgc.cat
xavier.goula@icgc.cat
teresasusagna@gmail.com

Manuscript received 20 July 2015;
Published Online 5 January 2016